SSRG International Journal of Electrical and Electronics Engineering
ISSN: 2348-8379/ https://doi.org/10.14445/23488379/IJEEE-V12I1P107

Volume 12 Issue 1, 63-75, January 2025

Original Article

Investigation of Particle Swarm Optimization Based Power System Stabilizer on Damping Performance in Two Area System with Voltage Dependent Load Models

Ghousul Azam Shaik[1], Lakshmi Devi Aithepalli[2]

[1,2]Department of Electrical and Electronics Engineering, Sri Venkateswara University, Andhra Pradesh, India.

[1]Corresponding Author : ghousul1993@gmail.com

Received: 04 November 2024 Revised: 06 December 2024 Accepted: 08 January 2025 Published: 25 January 2025

***Abstract* -** *This manuscript covers the impact of Particle Swarm Optimization (PSO) based Power System Stabilizer (PSS) on the damping performance in a two-area system with different voltage-dependent load models, including large-scale electric vehicle loads. In the first part of the design, the location of PSS was fixed by the procedure outlined in the manuscript and the later part of the design, PSO-PSS was proposed to tune the gain and time constant of the stabilizer by taking appropriate fitness function in Kundur two area four machine system. The PSO-based PSS designed for constant power type of load in the above system was placed at appropriate locations for other voltage-dependent load models. A comparison of damping ratios of inter-area mode was made with and without the stabilizer, and it was observed that the damping ratio of all inter-area modes with PSS was obtained by more than 3%. The results demonstrate that for both non-contingency and contingency of tie line in the above system, the PSO-based PSS designed for constant power type of load improved not only the damping ratio of inter-area mode but also increased the damping ratios of the other swing modes, including large scale electric vehicle loading case.*

***Keywords* -** *Inter-area mode, Linearization, Load modelling, Particle Swarm Optimization, Root locus.*

1. Introduction

The urge to use Electric Vehicles (EVs) to promote green energy is increasing day by day, but the stability of the grid employing the above needs to be studied thoroughly. In the current scenario, electric vehicles are acting both like loads as well as sources to power the grid. In past research works, the problem of signal stability improvement dealt with only modelling loads with constant impedances to make analysis simple and elegant. However, with the inclusion of nonlinear models, the analysis becomes complicated and thus needs to be addressed. In this manuscript, the effect of various types of load models on the small signal stability is dealt with systematically.

A supplementary controller like PSS needs to be installed along with the Automatic Voltage Regulators (AVR) in order to improve the damping of the various electromechanical modes in multi-area power systems. The procedure for finding the eigenvalues of the overall system matrix by taking up the concept of linearization of all the differential equations of machines, AVRs, PSS, algebraic equations of stators, transmission networks and loads was enlightened in [1, 2]. To introduce damping to rotor oscillations in Single Machine Infinite Bus System (SMIB), Chaotic PSO-based Proportional Integral Derivative (PID) PSS was prosed, and its performance was verified under light, nominal and heavy loading conditions [3]. The SMIB system was considered purely reactive.

Several operating conditions, such as different loading and network outages, were considered when designing robust PSS controller gains using sequential linear programming [4]. Participation factor analysis to determine the sensitivity of the electromechanical mode damping for optimal location was mentioned in [5]. Details of optimal PSS having a traditional phase lead-lag controller using LQR theory were given in [6]. Hybrid PSO and bacterial foraging methods for optimal PSS design to improve the small signal stability over a wide range of loading were discussed in [7].

Several PSS tuning rules using multi-objective optimization methods based on large signal disturbances behaviour on the Kundur two-area system are seen in [8]. The impact of various types of load models like Constant Power (CP), Constant Current (CI) and Constant Impedance (CZ) on the various electromechanical modes and exciter modes by assuming the transmission network in the quasi-steady state in the Western States Coordinating Council System was exhaustively studied by [1]. A small signal stability toolbox for designing PSS to damp low-frequency rotor oscillations in a system with partial data was used [9]. The authors presented conventional methods like root locus analysis for PSS design without any Artificial Intelligence (AI) technique in a two-generator Spanish system for improving the damping ratio of inter-area mode under different values of transmission line reactances. Exclusive information on power system stabilizer design methods in various single-machine and multi-machine systems using detailed small signal models and time domain simulation-based indices were presented by [10]. The details of using PSS in conjunction with various shunt/series compensators for the damping of rotor oscillations are presented in [11].

Eigenvalue analysis in two area systems with CZ load was presented in [12]. It considered participation factor analysis for placement of PSS considering all three tie lines in operation. The effect of the removal of tie lines in service was not considered in [12]. The authors of this paper deliberately have included such a scenario to assess small signal behaviour. The above analysis was done in Simulink-based software, and their eigenvalue analysis showed certain non-zero values, which are a part of numerical errors due to the linearization step. The authors of this manuscript have chosen to write MATLAB script instead of Simulink to ensure minimal numerical errors.

The eigenvalue approach to see the effect of load models on the oscillation damping in the Tai power system was seen in [13]. Details of dynamic, composite and exponential models, along with an overall comparison between them under line contingency, are in [13]. Details regarding the composition of residential, commercial and industrial loads are in [14]. Load flow solutions in distribution networks in the presence of EV are in [15]. The details regarding the small signal stability were not dealt with in [15].

Model Reference Adaptive Control (MRAC) PSS six to increase the small signal stability in the modified Kundur two-area system having wind power plants was proposed by [16]. The effect of EV load integration was not considered. The impact of EV modelling on low-frequency oscillations in a single machine system connected to a distribution system was studied by [17].

In this manuscript, the effect of EVs on the small signal stability in the grid was analysed with AVR only and with AVR and PSS. Some related work on the above was dealt with by [17] on a single-machine system. Performance of various AI-based PSS giving maximization of minimum damping ratio as an objective on SMIB and multi-machine systems using latent value analysis as a tool was elaborated in [18]. They did not study the impact of load models on several damping ratios. Papers [16-19] recommend reviews of PSS developments and their optimization routines. Based on the literature presented above, the following questions are posed to fill the research gaps.

- The PSS designed for a specific type of load representation (say, CP type) caters some damping to the inter-area mode for different types of voltage-dependent loads, including EV load?
- How does the damping ratio of swing modes of each area get affected in doing so?
- Where should the PSS be placed if voltage-dependent loads are taken into custody without using participation factor analysis?
- How should the PSS gain and time constant be tuned in a system when there is a loss of one of the tie lines?

In order to address the above questions, maximization of the sum of damping ratios of all modes was taken into consideration as an objective function to PSO in this manuscript with the intuition to not only increase the inter-area mode damping but also improve other swing mode damping ratios as well. This kind of fitness function was inspired by the works presented by [19].

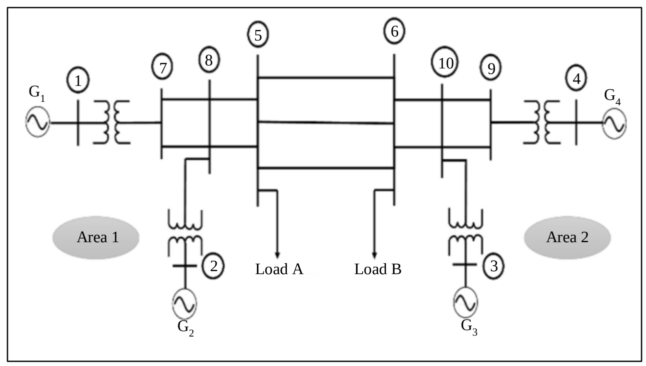

Fig. 1. One-line diagram of Kundur two-area system

The specific objectives of this study are:

1. To find the optimal location of PSS in the Kundur two-area system (Figure 1), various load models were used without the participation factor method.
2. To study the impact of PSS on the behaviour of inter-area mode.
3. To present the improvement of damping of inter-area mode by properly placing the PSS and tuning parameters like gain and time constant using the PSO technique for various scenarios and cases.

The following cases and scenarios have blossomed to provide a detailed view into the investigation of damping performance with PSO-PSS in the system by modelling loads - A and B as:

Case 1: Constant Power (CP)
Case 2: Constant Current (CI)
Case 3: Constant Impedance (CZ)
Case 4: Industrial load expressed by ZIP
Case 5: EVs modelled as ZIP

The small signal stability program was run for all the above five cases after doing load flow to get steady-state values of machines and network variables by generating scenarios in which:

Scenario 1: All three tie lines in service
Scenario 2: Two tie lines in service

The notation penned in [20] is adhered to here.

2. Problem Formulation

The inter-area modes, which are typically below 1 Hz frequency, arise in multi-machine systems. In order to provide damping to these modes, PSS has to be placed at the desired generator. Tuning of the same has to be done. So, a two-stage lead-lag PSS is proposed, whose details are in Section 2.1.

The first lead block gives phase lead whose time constants are T_1 and T_2 respectively in Figure 2. The washout time constant T_Q is fixed to be 10 s as the damping of inter-area mode is of prime concern.

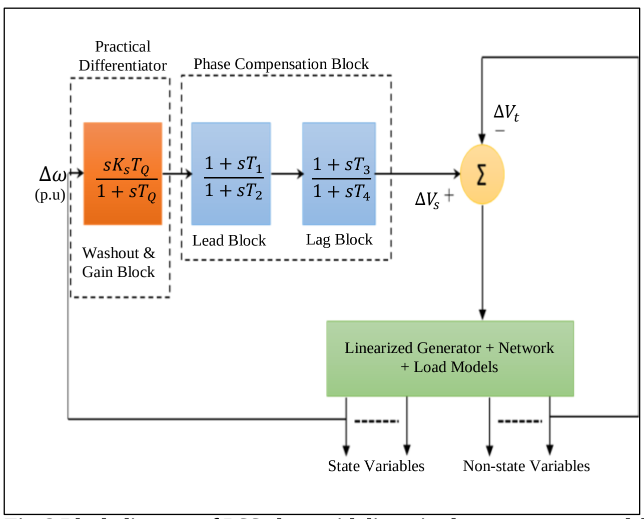

Fig. 2 Block diagram of PSS along with linearized power system model

The second lag block of fixed time constants T_3 and T_4 as in Figure 1 is kept to check overcompensation. The problem boils down to tuning K_s and T_1 if T_2 is fixed. This is done using the PSO technique, which takes FF as a fitness function for minimization.

$$FF = 1 - (\sum_{i=1}^{n} \zeta_i) \tag{1}$$

In Equation (1), 'n' is the total number of eigenvalues and 'ζ_i' is the damping ratio of i^{th} eigenvalue after placing PSS of tunable parameters K_s and T_1 where, $K_{s,min} \leq K_s \leq K_{s,max}$ and $T_{1,min} \leq T_1 \leq T_{1,max}$. The justification of FF is that Equation (1) takes into account all 'ζ_i' values. Fitness functions suggested in [18], like the min (max) function, allow only a single mode to be taken into account for damping.

2.1. Structure of PSS

PSS is a supplementary damping controller which is installed to counteract negative damping torque developed due to the voltage control action of AVR. A typical PSS block consists of a practical differentiator block, a gain block, and a lead-lag compensator block in tandem. The output of the PSS block is added to the summing point where modulation of voltage reference to AVR occurs. More insight into the synthesis of various control signals that can be fed as an input to PSS to provide positive damping to low-frequency oscillations is given in [21]. In this study, $\Delta\omega$ based PSS is employed, as shown in Figure 2.

2.2. Load Modelling

For performing a load flow study, it is customary to treat loads as CP type. CP type finds application in commercial areas. Residential areas mostly have CZ loads. However, for small signal stability studies, it is necessary to consider different types of voltage-dependent load models. They can be either exponential, ZIP or dynamic type.

Here, only 1st two types of load models were taken [see Equations (2)-(7)]. The values of α and β are 0, 0 for CP type, 1, 1 for CI type, 2 and 2 for CZ type, respectively. α_p, β_p, γ_p, α_q, β_q, γ_q values are 1.41, -1.61, 1.21, 3.72, -7.08, 4.35 for industrial loads and -0.1773, 0.9949, 0.1824, 4.993, -12.910, 8.917 for EV loads respectively. The nomenclature and constants in Equations (2), (3) are as per [22], whereas Equations (4)-(7) are from [14].

$$P = P_0 \left(\frac{V}{V_0}\right)^{\alpha} \tag{2}$$

$$Q = Q_0 \left(\frac{V}{V_0}\right)^{\beta} \tag{3}$$

$$P = P_0 \left[\alpha_p + \beta_p \left(\frac{V}{V_0}\right) + \gamma_P \left(\frac{V}{V_0}\right)^2\right] \tag{4}$$

$$Q = Q_0 \left[\alpha_q + \beta_q \left(\frac{V}{V_0}\right) + \gamma_q \left(\frac{V}{V_0}\right)^2\right] \tag{5}$$

$$\alpha_p + \beta_p + \gamma_p = 1 \tag{6}$$

$$\alpha_q + \beta_q + \gamma_q = 1 \tag{7}$$

3. PSO Optimization Technique

The overall flow chart combining the analytical method of small signal stability with PSO-based PSS is depicted in Figure 3. PSO, a metaheuristic algorithm, was developed by [23] inspired by the social activity of birds. PSO considers a swarm of particles, particles being spread over the minimum and maximum range in the plane. These particles are driven by giving an initial velocity. Velocity in subsequent steps is adjusted according to inertial weights. Each particle recollects its previous best position (Pbest), directs its velocity, and converges towards the global best position (Gbest).

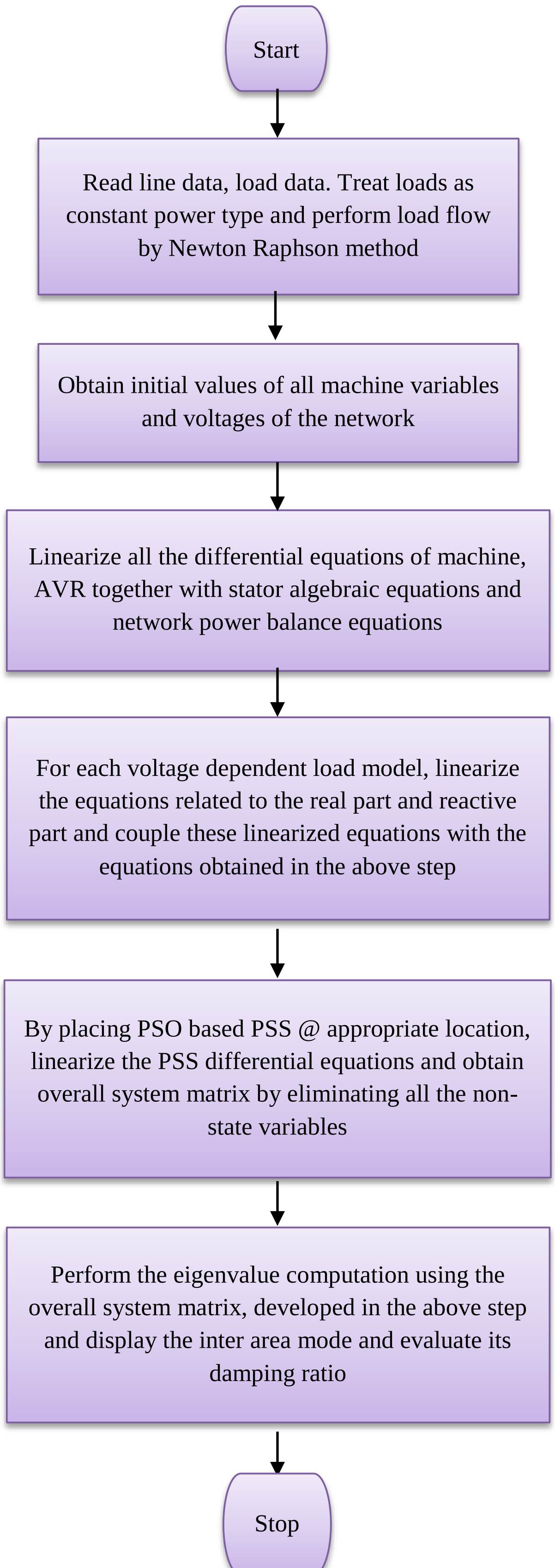

Fig. 3 Flow chart for scenario 1 and scenario 2

Let the swarm size and dimension be denoted by 'N' and 'D', respectively. Swarm 'X' is $X=[X_1,X_2,\ldots X_N]^T$. Each particle X_i is written as $X_i=[X_{i,1},X_{i,2},\ldots X_{i,D}]$ velocity $V=[V_1,V_2,\ldots V_N]^T$. Where $V_i=[V_{i,1},V_{i,2},\ldots V_{i,D}]$; i is from 1 to N and j is from 1 to D.

$Pbest_{i,j}^k$ is the personal best of j^{th} component of i^{th} particle in k^{th} iteration. $Gbest_j^k$ is j^{th} component of best individual till the k^{th} iteration. Particles are perturbed in each iteration by assigning the velocity as follows:

$$V_{i,j}^{k+1} = WV_{i,j}^k + C_1 r_1\left[Pbest_{i,j}^k - X_{i,j}^{k+1}\right] + C_2 r_2\left[Gbest_{i,j}^k - X_{i,j}^{k+1}\right] \quad (8)$$

Where r_1 and r_2 are random numbers in (0, 1); C_1 & C_2 are individual and social acceleration coefficients.

The inertial weight (W) is given as,

$$W = W_{max} - \frac{k}{k_{max}}(W_{max} - W_{\min}) \quad (9)$$

Details regarding the PSO Algorithm are given below, followed by the flow chart in Figure 4.

3.1. PSO Algorithm

Step 1: Initialize all the PSO parameters.

$N=30$, $k_{max}=600$, $W_{min}=0.4$, $W_{max}=0.9$, $C_1=2$, $C_2=2$

Step 2: Set iteration count (K) =1

Step 3: Assuming X ranging X_{min} to X_{max}, generate random positions (initially) as,

$$X = X_{min} + rand[X_{max} - X_{min}] \quad (10)$$

Assume the initial velocity to be 1% of X.

Step 4: Find $F_i^k = F\left(X_{i,j}^k\right)\forall$ 'i'. Find the index of best particle b (where b ε i)

Step 5: Initialize $Pbest_{i,j}^k = X_i^k$ and $Gbest_j^k = X_b^k$

Step 6: Find W from (9) and calculate $V_{i,j}^{k+1}$ from (8) and update $X_{i,j}^{k+1}$ as $X_{i,j}^k + V_{i,j}^{k+1}$

Step 7: Evaluate $F_i^k = F\left(X_{i,j}^k\right)\forall$ particles 'i' to find the index of the best particle b_1

Step 8: For ∀ the particle 'i' update the Pbest as follows.

If $F_i^{k+1} < F_i^k$ then set $Pbest_i^{k+1} \to X_i^{k+1}$, Else $Pbest_i^{k+1} \to Pbest_i^k$

Step 9: Update Gbest as follows.

If $F_{b1}^{k+1} < F_b^k$ then set $Gbest_i^{k+1} \to Pbest_i^{k+1}$ and do $b \to b_1$

Else $Gbest^{k+1} \to Gbest^k$ and Set k=k+1 and run the program till $k=k_{max}$.

Step 10: Print $Gbest^k$

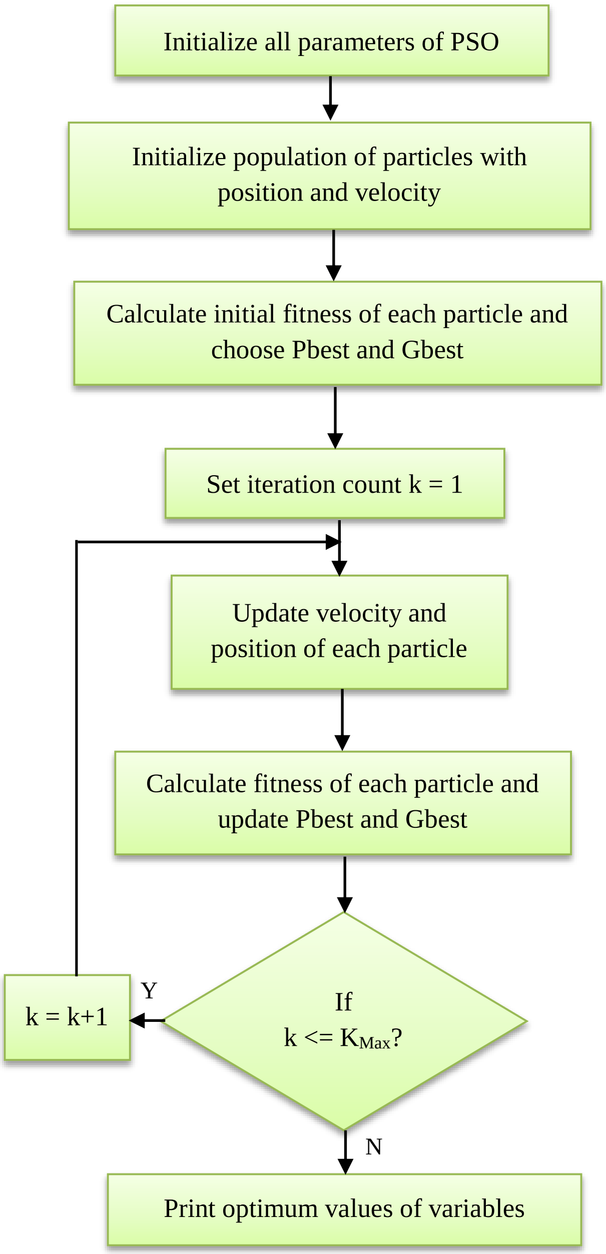

Fig. 4 Flow chart of PSO algorithm

4. Results and Discussions

The system with 'X' generators has '$(X-1)$' electromechanical modes. Kundur two area system has four generators, ten nodes, two loads and three tie lines. By modelling loads as constant power, the scripting of the polar version of Newton Raphson load flow was done in the MATLAB 2020 environment, which served as an input to the eigenvalue analysis of the MATLAB script.

Kundur two area system data was taken from [21] in which the mechanical damping of the machine is given as 0. However, in this work, it is taken as 0.01 for all machines. The validation of MATLAB code for small signal stability analysis was done by writing the program on the data given in [21], and eigenvalues were obtained very accurately with the values presented in [21]. [21] dealt only with modelling loads as CZ type only, i.e. case 3 scenario 1. This confirms the validity of MATLAB code developed for CZ type, which can be changed to incorporate new cases and scenarios.

4.1. Scenario 1 without PSS

The results of the eigenvalue analysis for each case with AVR only are shown in Figure 5. Swing mode 3 is the inter-area mode and is of specific interest to us, as seen in Table 1. Damping of inter-area mode for cases 1-5 are 0.96, 0.67, 0.46, 0.81 and 0.92 % respectively, for scenario 1, which are less than 3.0 %. The other swing modes have a damping ratio of more than 10% for all the cases of scenario 1, as shown in Table 1. It was suggested in [24] that a minimum damping ratio of 0.03 is acceptable for power system operation under stressed situations.

4.2. Placement of PSS for Scenario 1

The time constants T_1, T_2, T_3, and T_4 and were fixed as 0.047, 0.0218, 3.0, 5.4 s, respectively given in [21], and PSS gain was varied from 0 to 30 by locating PSS at each generator. Among four generator sites, the location for which the locus is away from the imaginary axis is considered the selection criterion for the location of PSS. G_1 was found to be the candidate node for case 1, whereas, for cases 2-5, G_4 was found to be a desirable node for placing the same, as seen in Figure 6.

4.3. Tuning of PSS for Scenario 1

For case 1, with the location fixed in the previous step, K_s and T_1 were selected as tunable parameters by giving FF as an objective function to the PSO algorithm for minimization, whose parameters are given in Section 3.

The PSS parameters tuned by PSO are K_s=17.2079 and T_1=0.2472 for case 1. The remaining parameters (T_2, T_3, T_4 and T_Q) of PSS are left undisturbed. The small signal stability program was rerun by including PSS at G_1. It was observed that all swing mode damping ratios increased when compared to the base case shown in Table 1 for case 1.

All eigenvalues corresponding to scenario 1 for cases 1-5 after placing PSS are shown in Figure 7. The real part of the swing mode-3 drifted away from the imaginary axis for cases 1-5, as tabulated in Table 1.

The improvement of the damping ratio of swing mode- 3 by placing PSS at G_1 for CP type of loading is from 0.96 to 5.72% as given in Table 1. By placing PSS at G_4, the improvement of the damping ratio of swing mode-3 for cases 2-5 is from 0.67 to 4.48, 0.46 to 4.87, 0.81 to 4.47, and 0.92 to 5.08%, respectively, as in Table 1.

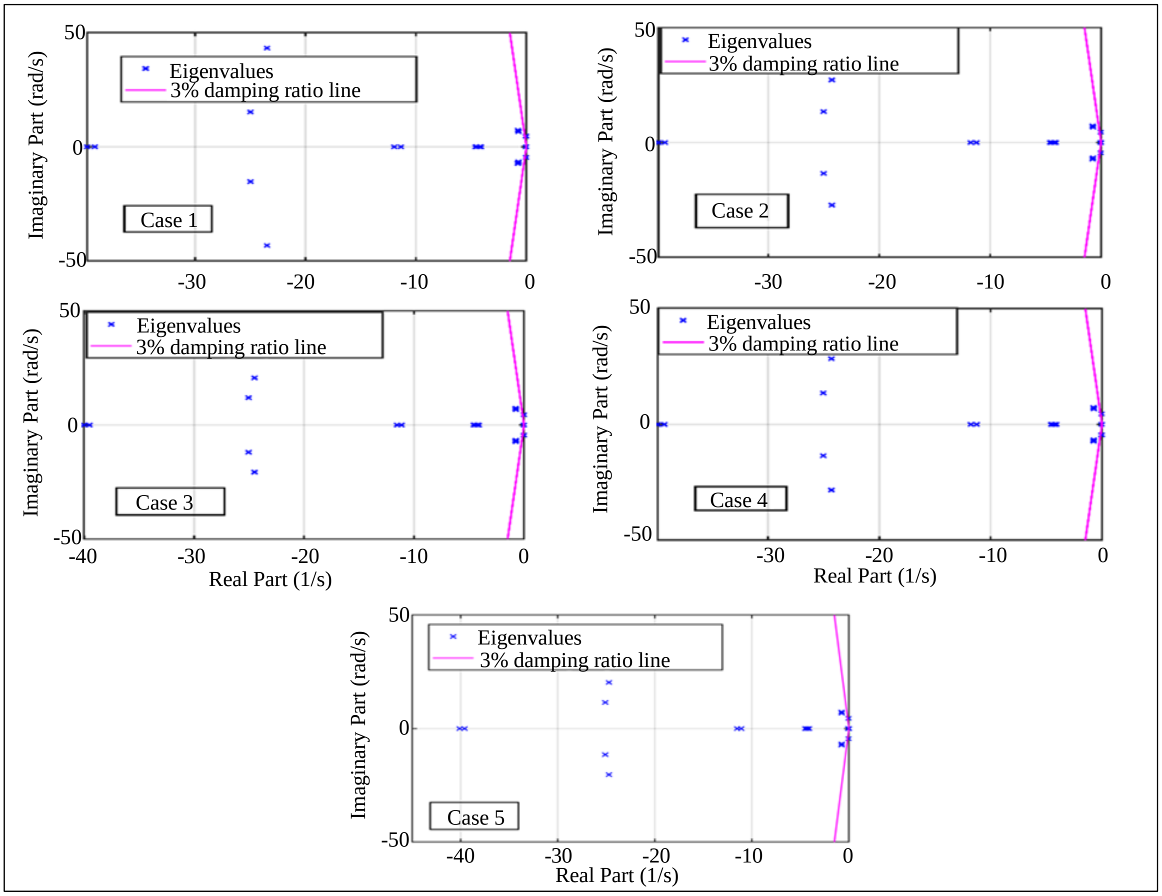

Fig. 5 Eigenvalue plots without PSS of inter-area modes for cases 1- 5 corresponding to scenario 1

Table 1. The damping ratio of various electromechanical modes before and after placing PSO based PSS corresponding to scenario 1

Case	Swing Mode	Eigenvalue		Damping Ratio, %	
		Without PSS	With PSS	Without PSS	With PSS
1	1	-0.7680 ± j 7.2818	-2.2872 ± j 6.5073	10.49	33.16
	2	-0.7179 ± j6.6473	-0.7385 ± j 6.6537	10.74	11.03
	3	-0.0441 ± j4.6056	-0.2615 ± j 4.5606	0.96	5.72
2	1	-0.7724 ± j 7.3023	-0.7721 ± j 7.3016	10.52	10.52
	2	-0.7406 ± j 6.6842	-1.9791 ± j 6.1001	11.01	30.86
	3	-0.0305 ± j 4.5260	-0.2009 ± j 4.4803	0.67	4.48
3	1	-0.7738 ± j 7.3186	-0.7737 ± j 7.3182	10.51	10.51
	2	-0.7502 ± j 6.7123	-1.9075 ± j 6.1765	11.11	29.51
	3	-0.0207 ± j 4.4572	-0.2143 ± j 4.3937	0.46	4.87
4	1	-0.7705 ± j 7.2997	-0.7702 ± j 7.2989	10.50	10.49
	2	-0.7361 ± j 6.6799	-1.9961 ± j 6.0788	10.95	31.20
	3	-0.0366 ± j 4.5440	-0.2015 ± j 4.5041	0.81	4.47
5	1	-0.7672 ± j 7.3164	-0.7670 ± j 7.3101	10.43	10.43
	2	-0.7394 ± j 6.7112	-1.9328 ± j 6.1438	10.95	30.01
	3	-0.0410 ± j 4.4975	-0.2263 ± j 4.4486	0.92	5.08

Table 2. Damping ratio of various electromechanical modes before and after placing PSO-based PSS corresponding to scenario 2

Case	Swing Mode	Eigenvalue		Damping Ratio, %	
		Without PSS	With PSS	Without PSS	With PSS
1	1	-0.7622 ± j 7.2502	-2.2518 ± j 6.7571	10.45	31.62
	2	-0.7064 ± j 6.6253	-0.7154 ± j 6.6263	10.60	10.73
	3	-0.0332 ± j 4.0895	-0.1694 ± j 4.0517	0.81	4.18
2	1	-0.7682 ± j 7.2739	-0.7680 ± j 7.2734	10.50	10.50
	2	-0.7309 ± j 6.6636	-1.9237 ± j 6.2816	10.90	29.28
	3	-0.0160 ± j 3.9981	-0.1267 ± j 3.959	0.40	3.20
3	1	-0.7706 ± j 7.2924	-0.7705 ± j 7.2922	10.51	10.51
	2	-0.7417 ± j 6.6927	-1.8540 ± j 6.3439	11.01	28.05
	3	-0.0039 ± j 3.9199	-0.1432 ± j 3.8634	0.10	3.70
4	1	-0.7659 ± j 7.2708	-0.7658 ± j 7.2705	10.48	10.47
	2	-0.7260 ± j 6.6588	-1.9405 ± j 6.2648	10.84	29.59
	3	-0.0228 ± j 4.0200	-0.1258 ± j 3.9862	0.57	3.15
5	1	-0.7631 ± j 7.2902	-0.7630 ± j 7.2900	10.41	10.41
	2	-0.7303 ± j 6.6911	-1.8793 ± j 6.3202	10.85	28.50
	3	-0.0251 ± j 3.9712	-0.1496 ± j 3.9296	0.63	3.80

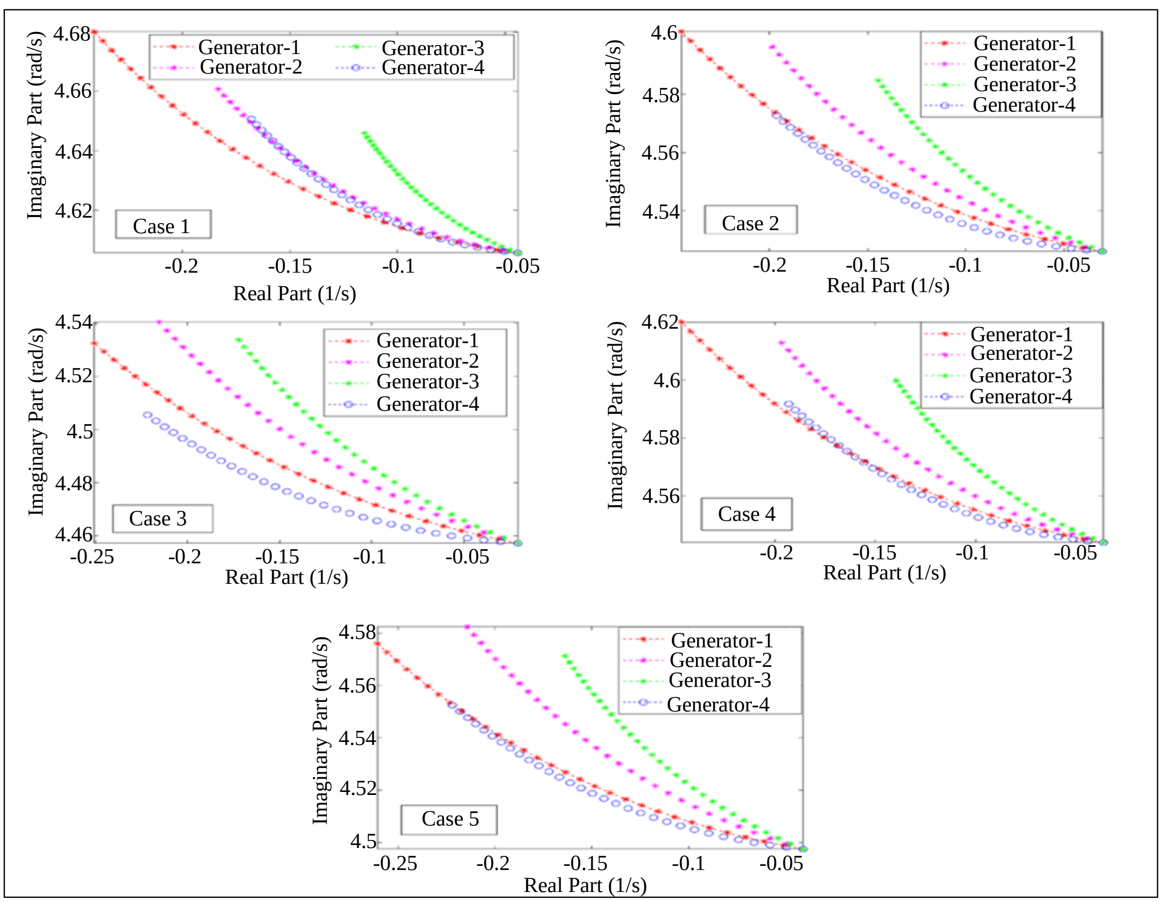

Fig. 6 Root locus plots of inter-area modes for cases 1-5 corresponding to scenario 1

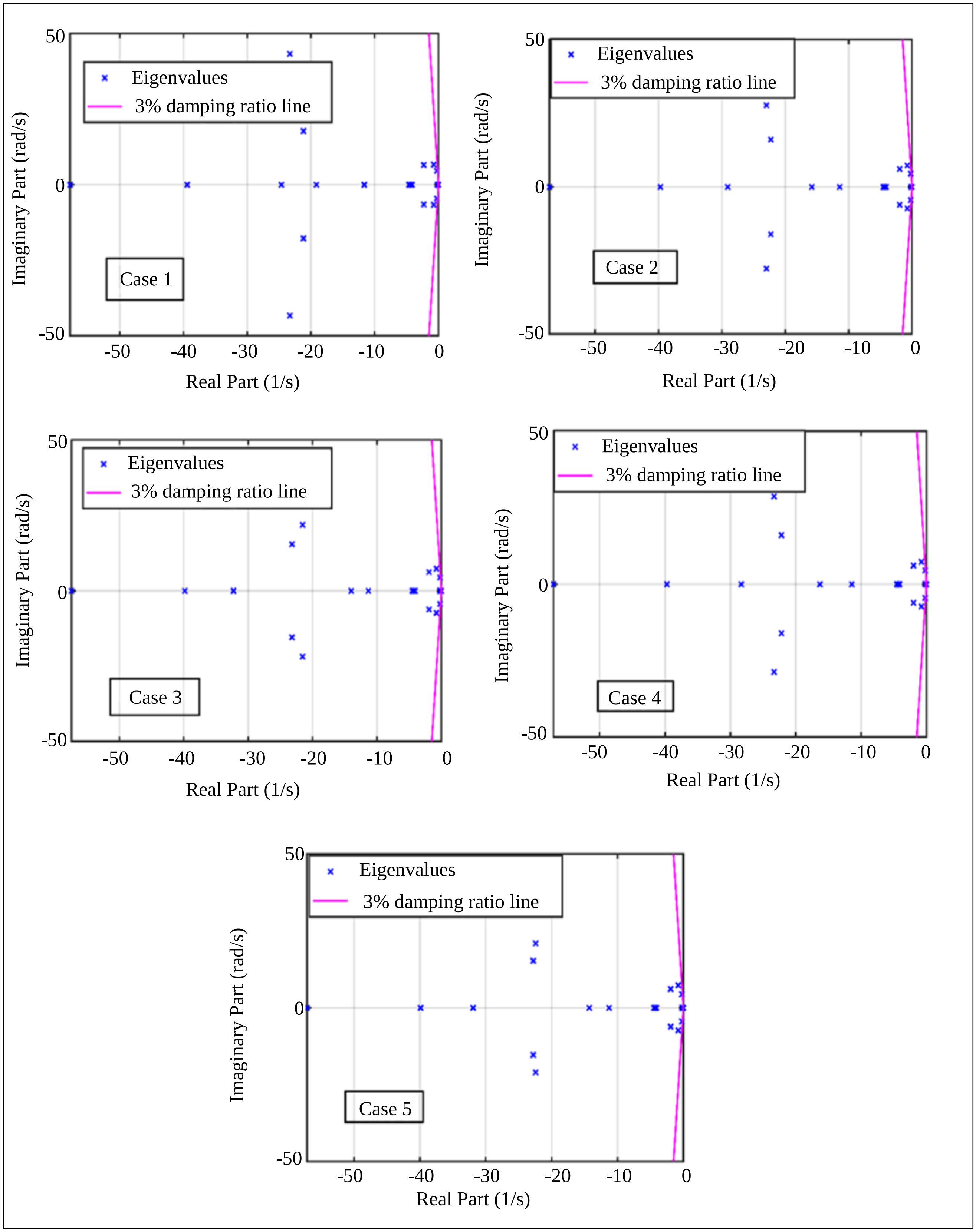

Fig. 7 Eigenvalue plots of inter-area modes with PSS for cases 1-5 corresponding to scenario 1

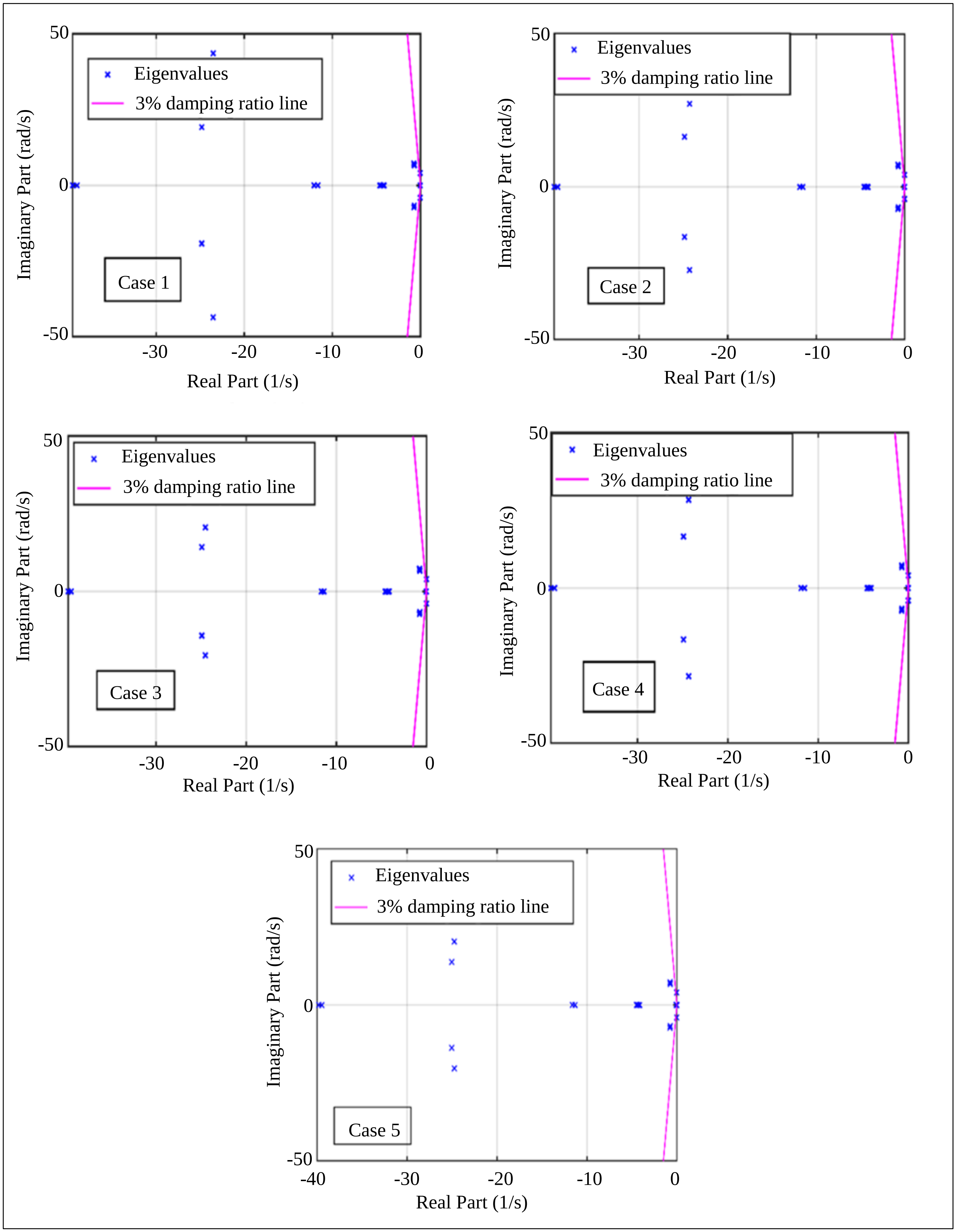

Fig. 8 Eigenvalue plots for cases 1-5 corresponding to scenario 2 without PSS

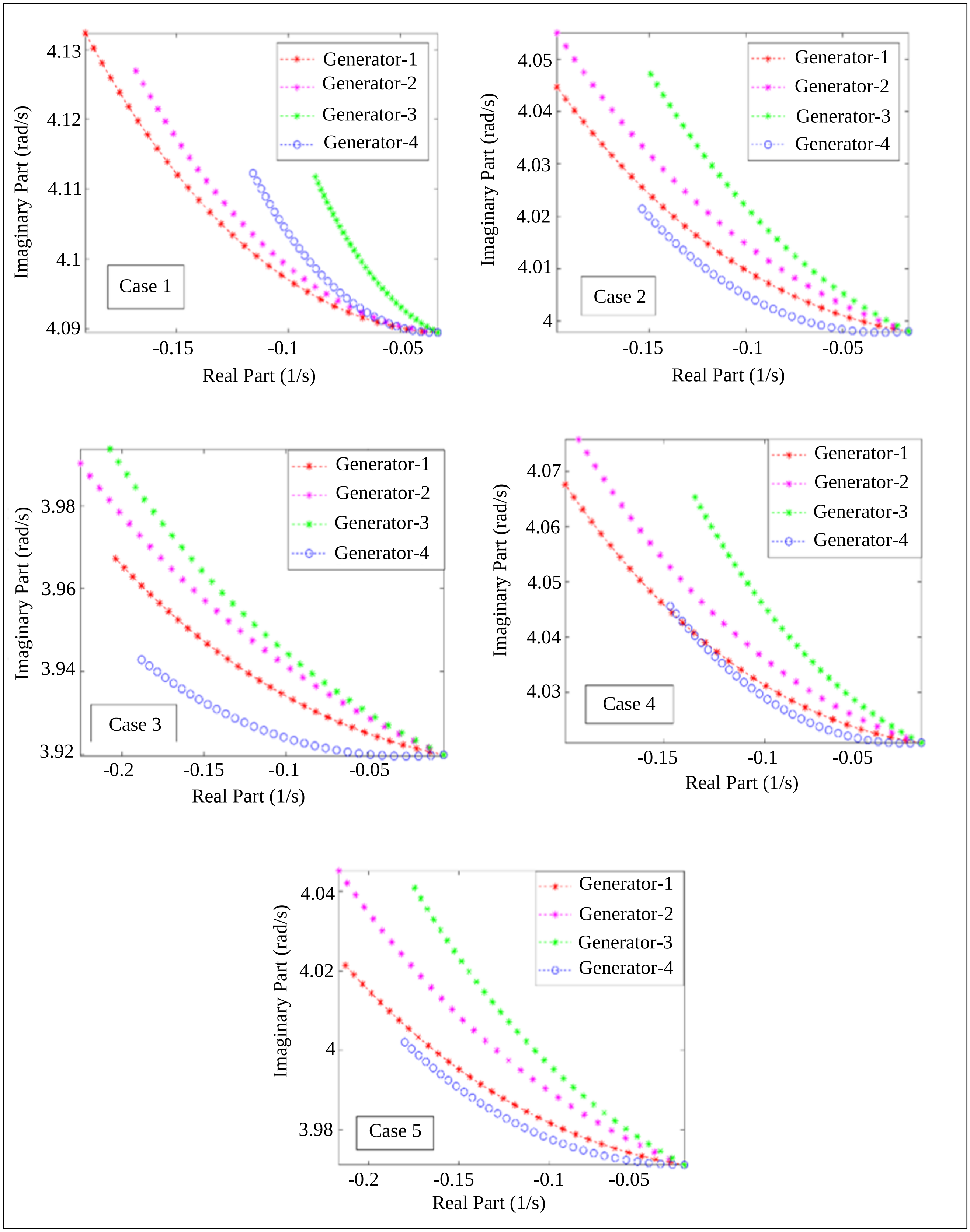

Fig. 9 Root locus plots of inter-area modes for cases 1-5 corresponding to scenario 2

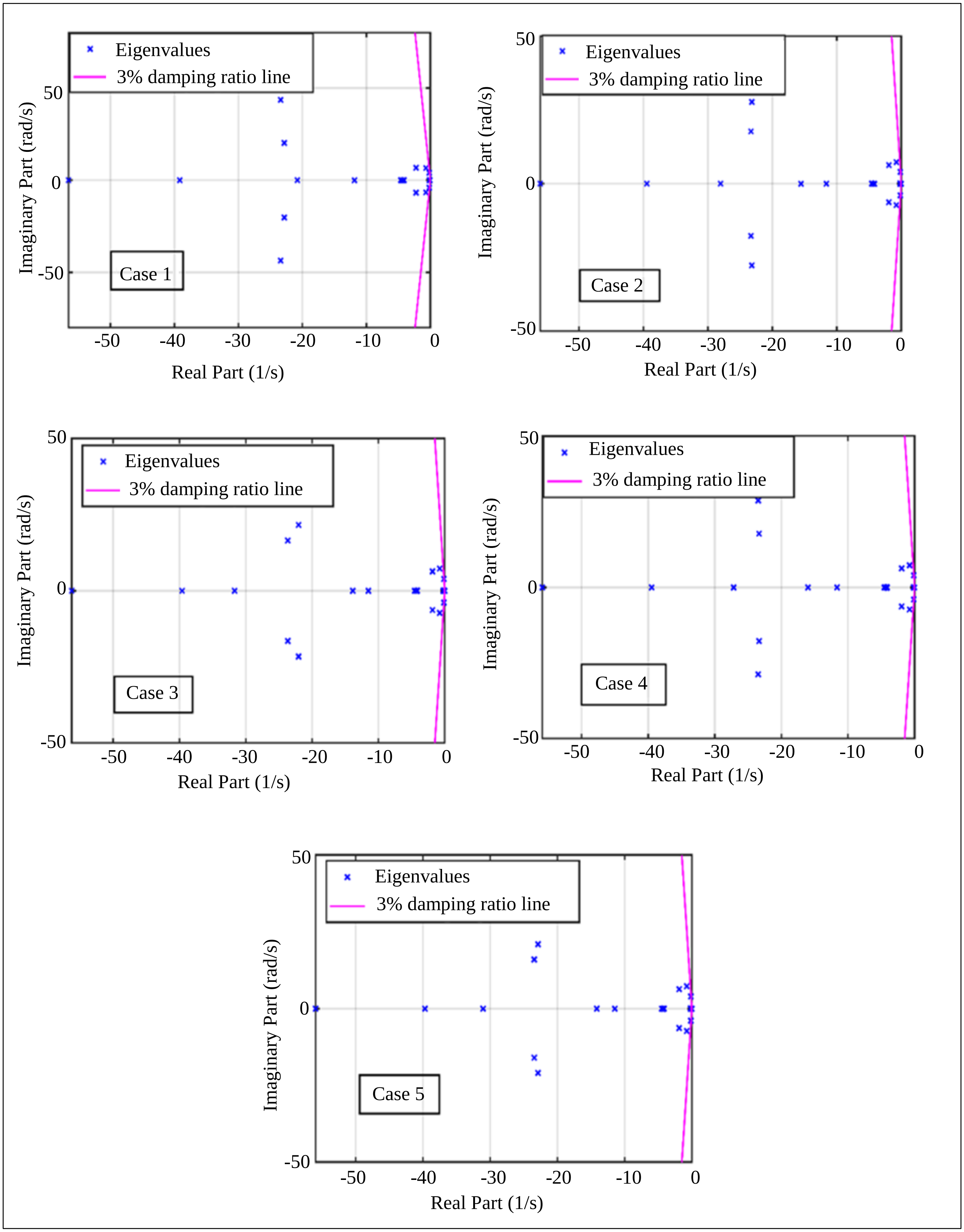

Fig. 10 Eigenvalue plots with PSS for cases 1-5 corresponding to scenario 2

4.4. Scenario 2 without PSS

The load flow program was rerun by removing one tie line between 5th and 6th nodes. The results of eigenvalue analysis for each case with AVR only are shown in Figure 8. The damping of the inter-area mode (swing mode - 3) for cases 1-5 are 0.81, 0.40, 0.10, 0.57 and 0.63 % respectively for scenario 2. It is evident from the above results that for all the above cases, the damping ratio of swing mode 3 is less than 1.0 %. It was found that the damping ratio of the inter-area mode deteriorated when compared to scenario 1. The other swing modes have a damping ratio of more than 10% for all the cases of scenario 2, as shown in Table 2.

4.5. Placement of PSS for Scenario 2

The procedure outlined in Section 4.2 is followed, and from Figure 9, G_1 was found to be the candidate node for case 1, and G_4 was found to be a desirable node for cases 2-5 for placing PSS.

4.6. Tuning of PSS for Scenario 2

Locating PSS at G_1, K_s and T_1 were tuned by PSO algorithm to obtain K_s as 16.6370 and T_1 as 0.2173 s for case 1. The remaining parameters (T_2, T_3, T_4 and T_Q) of PSS are left undisturbed. The program was rerun by including PSS at G_1. It was observed that all the swing mode damping ratios increased when compared to the base case shown in Table 2 for case 1.

All eigenvalues corresponding to scenario 2 for cases 1-5 after placing PSS are shown in Figure 10. The real part of the critical inter-area mode has drifted away from the imaginary axis for all cases 1-5, as tabulated in Table 2. Improvement of the damping ratio of swing mode 3 by placing PSS at G_1 for CP type is from 0.81 to 4.18%, as seen in Table 2. By placing PSS at G_4, the improvement of the damping ratio of swing mode-3 for cases 2-5 is from 0.40 to 3.20, 0.10 to 3.70, 0.57 to 3.15, and 0.63 to 3.80 %, respectively (Table 2).

Although PSS was located at G_4 for cases 2-3, there is no significant difference in the percentage damping ratio of swing mode-1, whereas a slight decrease in case 4 was seen. For case 5, all the swing modes increased for the Scenario 2. Thus, from Tables 1 and 2, it can observed that EV integration into the system instead of CC, CZ and Industrial type has benefitted the inter-area mode damping along with the proposed PSS.

5. Conclusion and Future Work

The proposed PSO-PSS has improved the damping ratio of the inter-area mode by more than 3% for both non-contingency and contingency cases for all load models. Since the fitness function to PSO is the sum of the damping ratios of all modes, it was observed from the results that in addition to improving the damping of inter-area mode, the other swing modes were also improved in most of the cases for both non-contingency and contingency of the tie line scenarios. After placing PSS, the highest damping ratio for inter-area mode was recorded for the EV load model when compared to CC, CZ and Industrial load models.

Funding Statement

Ghousul Azam Shaik thanks the University Grants Commission (UGC), New Delhi, India, for providing a Junior Research Fellowship during the PhD program with grant number 220510236223.

References

[1] Rajeev K. Ranjan, M.A. Pai, and P.W. Sauer, “Analytical Formulation of Small Signal Stability Analysis of Power Systems with Nonlinear Load Models,” *Sadhana*, vol. 18, pp. 869-889, 1993. [CrossRef] [Google Scholar] [Publisher Link]

[2] Mark J. Laufenberg, M.A. Pai, and K.R. Padiyar, “Hopf Bifurcation Control in Power Systems with Static Var Compensators,” *International Journal of Electrical Power & Energy Systems*, vol. 19, no. 5, pp. 339-347, 1997. [CrossRef] [Google Scholar] [Publisher Link]

[3] Ayad Fadhil Mijbas et al., “Optimal Stabilizer PID Parameters Tuned by Chaotic Particle Swarm Optimization for Damping Low Frequency Oscillations (LFO) for Single Machine Infinite Bus System (SMIB),” *Journal of Electrical Engineering, and Technology*, vol. 15, no. 4, pp.1577-1584, 2020. [CrossRef] [Google Scholar] [Publisher Link]

[4] Rabih A. Jabr, Bikash C. Pal, and Nelson Martins, “A Sequential Conic Programming Approach for the Coordinated and Robust Design of Power System Stabilizers,” *IEEE Transactions on Power Systems*, vol. 25, no. 3, pp. 1627-1637, 2010. [CrossRef] [Google Scholar] [Publisher Link]

[5] Debasish Mondal, “A Unique Method for Selection of Optimum Location of Power System Stabilizer to Mitigate Small-Signal Stability Problem,” *The Institution of Engineers (India)*, vol. 91, pp. 14-20, 2010.

[6] Jawad Talaq, “Optimal Power System Stabilizers for Multi Machine Systems,” *International Journal of Electrical Power & Energy Systems*, vol. 43, no. 1, pp. 793-803, 2012. [CrossRef] [Google Scholar] [Publisher Link]

[7] S.M. Abd-Elazim, and E.S. Ali, “A Hybrid Particle Swarm Optimization and Bacterial Foraging for Optimal Power System Stabilizers Design,” *International Journal of Electrical Power & Energy Systems*, vol. 46, pp. 334-341, 2013. [CrossRef] [Google Scholar] [Publisher Link]

[8] Baraa Mohandes, and Youssef L. Abdelmagid, and Igor Boiko, “Development of PSS Tuning Rules Using Multi-objective Optimization,” *International Journal of Electrical Power & Energy Systems*, vol. 100, pp. 449-462, 2018. [CrossRef] [Google Scholar] [Publisher Link]

[9] J. Renedo, L. Sigrist, and L. Rouco, "Design of Power System Stabilizers to Damp Low Frequency Inter-Area Oscillations with Limited Information," *2019 IEEE Milan PowerTech*, Milan, Italy, pp. 1-6, 2019. [CrossRef] [Google Scholar] [Publisher Link]

[10] Adrian Nocoń, and Stefan Paszek, "A Comprehensive Review of Power System Stabilizers," *Energies*, vol. 16, no. 4, 2023. [CrossRef] [Google Scholar] [Publisher Link]

[11] Ramesh Devarapalli, Nikhil Kumar Sinha, and Fausto Pedro García Márquez, "A Review on the Computational Methods of Power System Stabilizer for Damping Power Network Oscillations," *Archives of Computational Methods in Engineering*, vol. 29, no. 6, pp. 3713-3739, 2022. [CrossRef] [Google Scholar] [Publisher Link]

[12] Jarapala Siva Naik, R. Thirumalaivasan, and M. Janaki, "Analysis of Multi-Machine Power System with PSS Using Participation Factor Method," *2021 Innovations in Power and Advanced Computing Technologies (i-PACT)*, Kuala Lumpur, Malaysia, pp. 1-7, 2021. [CrossRef] [Google Scholar] [Publisher Link]

[13] Wen-Shiow Kao, "The Effect of Load Models on Unstable Low-Frequency Oscillation Damping in Tai power System Experience w/wo Power System Stabilizers," *IEEE Transactions on Power Systems*, vol. 16, no. 3, pp. 463-472, 2001. [CrossRef] [Google Scholar] [Publisher Link]

[14] Bablesh K. Jha et al., "A Modified Current Injection Load Flow Method under Different Load Model of EV for Distribution System," *International Transactions on Electrical Energy Systems*, vol. 30, no. 4, 2020. [CrossRef] [Google Scholar] [Publisher Link]

[15] Y. Kongjeen et al., "A Modified Backward and Forward Sweep Method for Microgrid Load Flow Analysis under Different Electric Vehicle Load Mathematical Models," *Electric Power Systems Research*, vol. 168, pp. 46-54, 2019. [CrossRef] [Google Scholar] [Publisher Link]

[16] Ping He et al., "Introducing MRAC-PSS-VI to Increase Small-Signal Stability of the Power System after Wind Power Integration," *International Transactions on Electrical Energy Systems*, vol. 2022, 2022. [CrossRef] [Google Scholar] [Publisher Link]

[17] Kulsomsup Yenchamchalit et al., "Control of Low-frequency Oscillation on Electrical Power System under Large EV-Charging Station Installation Using PSO Technique for Turning PSS Parameters," *International Review of Electrical Engineering*, vol. 16, no. 5, pp. 401-408, 2021. [CrossRef] [Google Scholar] [Publisher Link]

[18] Md. Rashidul Islam et al., "Power System Stability Enhancement through Optimal PSS Design," *e-Prime - Advances in Electrical Engineering, Electronics and Energy*, vol. 9, 2024. [CrossRef] [Google Scholar] [Publisher Link]

[19] Mohamad Almas Prakasa et al., "A Hybrid Controlling Parameters of Power System Stabilizer and Virtual Inertia Using Harris Hawk Optimizer in Interconnected Renewable Power Systems," *IEEE Access*, vol. 12, pp. 76219-76243, 2024. [CrossRef] [Google Scholar] [Publisher Link]

[20] Peter W. Sauer, M.A. Pai, and Joe H. Chow, *Power System Dynamics and Stability: With Synchrophasor Measurement and Power System Toolbox*, 2nd Ed., Wiley-IEEE Press, 1998. [Google Scholar] [Publisher Link]

[21] M.A. Pai et al., *Small Signal Analysis of Power Systems*, Narosa Publishing House, New Delhi, 2004. [Google Scholar] [Publisher Link]

[22] C. Concordia, and S. Ihara, "Load Representation in Power Systems Stability Studies," *IEEE Transactions on Power Apparatus and Systems*, vol. PAS-101, no. 4, pp. 969-977, 1982. [CrossRef] [Google Scholar] [Publisher Link]

[23] J. Kennedy, and R. Eberhart, "Particle Swarm Optimization," *Proceedings of ICNN'95- International Conference on Neural Networks*, Perth, WA, Australia, vol. 4, pp. 1942-1948, 1995. [CrossRef] [Google Scholar] [Publisher Link]

[24] Xi-Fan Wang, Yonghua Song, and Malcolm Irving, *Modern Power Systems Analysis*, Springer, New York, 2008. [CrossRef] [Google Scholar] [Publisher Link]